ASCE

Simulation Analysis of Pumping Characteristics for High-Altitude Concrete

Guoju Ke[1]; Bo Tian[2]; Yangtao Yuan[3]; Jun Zhang[4]; and Lihui Li[5]

Abstract: To investigate the characteristics of high-altitude concrete, the influences of atmospheric pressure on the air content, bubble stability, and pore structure of air-entrained concrete were tested by simulating a low-pressure condition using an environmental chamber. The pumping process was simulated using a resistance tester to investigate the effects of atmospheric pressure on the concrete slump, slump flow, V-funnel time, and pumping resistance. The results showed that the air content of air-entrained concrete decreases significantly with decreasing atmospheric pressure and that the pore structure of hardened concrete deteriorates. Among the admixture components, the effect of the air-entraining agent (AEA) on reducing concrete pumping resistance was the most evident. The pumping resistance of concrete increases at low atmospheric pressure, but that of concrete with AEA increases minimally. Combined with the ideal gas state equation, the air-entraining mechanism of high-altitude concrete was explained. **DOI: 10.1061/(ASCE)MT.1943-5533.0004002.** © *2021 American Society of Civil Engineers.*

Author keywords: High-altitude concrete; Low atmospheric pressure; Air-entraining performance; Pumping resistance; Air-entraining mechanism.

Introduction

The Qinghai-Tibet Plateau in China has an average elevation of over 3,500 m. It is known as the *roof of the world* and covers an area of 2.4 million km^2, thereby accounting for approximately one quarter of the country's land area. In general, for every 1,000 m of elevation, atmospheric pressure is reduced by approximately 10% (Li et al. 2015). Under high-altitude and low-pressure environmental conditions, the performance of cement concrete, particularly its air-entraining performance, is inevitably affected, which can cause changes in the pumpability of concrete (Vosahlik et al. 2018). Pumping is a mechanized process that can accelerate construction progress and improve the mobility of concrete transportation, even if the construction site is narrow. High-rise, large-volume, and long-span cement concrete structures are mostly poured by pumping. The pumpability of concrete indicates that concrete does not block a pipe or segregate in a pumpline. Difficulty in pumping is typically characterized by indicators such as slump, slump flow, and V-funnel time. To ensure the pumpability of cement concrete, adding admixtures, which are mostly composed of a water-reducing component, an air-entraining component, a retarding component, and a viscosity-increasing component, is generally necessary. A water-reducing agent ensures the workability of the pumped concrete; an air-entraining agent (AEA) is beneficial in reducing pumping resistance, thereby slowing concrete segregation and bleeding; and a retarder achieves concrete slump retention, particularly under high-temperature conditions during summer (Ke et al. 2015, 2020) and in the case of long-distance transportation (He and Hu 2006; Ke and Zhang 2020; Ke et al. 2020). In addition, some viscosity-modifying admixture (VMA) components are added to increase the viscosity of concrete without segregation and bleeding (Dhanapal and Nanthagopalan 2020; Georgiadis et al. 2010). Although indicators, such as slump, slump flow, and V-funnel time, can evaluate the pumpability of concrete to some extent, they are insufficiently intuitive to directly reflect the resistance of concrete in a pumpline. Accordingly, a cement concrete resistance tester for simulating pumping was developed (Ke et al. 2019), primarily to simulate the behavior of fresh concrete in a pumpline (Hazaree and Mahadevan 2016; Jacobsen et al. 2009; Liu et al. 2020; Wu et al. 2011; Yazdani et al. 2000) and determine the pumping resistance value of concrete, thereby directly reflecting the difficulty of pumping concrete (Feys et al. 2015; Kim et al. 2017). The effects of atmospheric pressure on the air-entraining performance and pore structure of concrete were studied. Simultaneously, the concrete pumping resistance of different admixture combinations under different atmospheric pressures was compared. The results were used as a reference for preparing and pouring concrete in high-altitude areas.

Experimental Program

Materials

The compressive strengths of ordinary portland cement 42.5 are 22.5 and 48.5 MPa at 3 and 28 days, respectively, and the corresponding flexural strengths are 4.9 and 8.8 MPa (Ke et al. 2019). Natural river sand from Dong Tianyang has a fine modulus of 2.7,

[1]Associate Research Fellow, Highway Engineering Research Center, Research Institute of Highway Ministry of Transport, Beijing 100088, China; Ph.D. Student, Dept. of Civil Engineering, Tsinghua Univ., Beijing 100084, China. ORCID: https://orcid.org/0000-0002-8585-1220. Email: keguoju@163.com

[2]Senior Researcher, Highway Engineering Research Center, Research Institute of Highway Ministry of Transport, Beijing 100088, China (corresponding author). Email: tbb73@yahoo.com

[3]Engineer, Air Force 95028, No. 518 Luoyu Rd., Hongshan District, Wuhan 430079, China. Email: floyd0201@163.com

[4]Professor, Dept. of Civil Engineering, Tsinghua Univ., Beijing 100084, China. Email: junz@tsinghua.edu.cn

[5]Associate Research Fellow, Highway Engineering Research Center, Research Institute of Highway Ministry of Transport, Beijing 100088, China. Email: lilihui0451@163.com

Note. This manuscript was submitted on April 24, 2020; approved on April 22, 2021; published online on October 21, 2021. Discussion period open until March 21, 2022; separate discussions must be submitted for individual papers. This paper is part of the ***Journal of Materials in Civil Engineering***, © ASCE, ISSN 0899-1561.

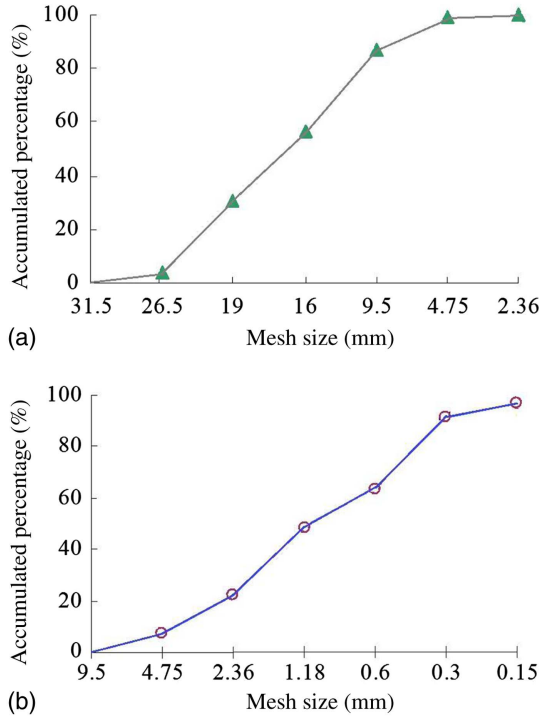

Fig. 1. Grading curves of aggregate: (a) limestone gravel; and (b) river sand.

continuous grading limestone gravel measured 5–25 mm, and the relevant grading curves are shown in Figs. 1(a and b). A Viscocrete3301C (water agent) Sika polycarboxylate water reducer with a water reduction rate of 25% was used (Sika Group, Beijing). Rosin heat polymer (RHP) and sodium dodecyl sulfate (SDS) AEAs were obtained from a company in Shanxi Province and recommended to be 0.02%–0.05% by weight of the cement for an air content of 3%–10% in concrete. Welan gum (WG) viscosifier was produced by Hebei Hengsheng. The retarder used was industrial-grade sodium gluconate (SG) with an effective content of 98%.

Mixture Proportions

The mixture proportions refer to C40 concrete, and the slump was greater than 120 mm, as given in Table 1. The water-to-cement ratio by mass was 0.4. Various chemical admixture contents (by mass of cement) were then added, as provided in Table 2, while keeping the preceding parameters unchanged.

Testing Procedures

Concrete Mixed Under Different Atmospheric Pressure Conditions

An LRHS-1000C-LF low-pressure test chamber (Fig. 2) (Shanghai Linpin Instrument Stock, Shanghai, China) was used with the following parameters: 1,000 × 1,000 × 1,000 mm in size, temperature range from −40°C to 150°C, and pressure range of 0.5–101 kPa. Normal- and low-pressure tests were performed in the low-atmospheric-pressure test chamber. The materials were fed in the following order: cement and sand, gravel, and additives and water. The mixer used was a double horizontal shaft forced mixer with a 10 L mixture per batch; the mixing rate was 60 rpm, and the mixing time was 120 s. The slump flow, V-funnel time, air content, and pumping resistance were immediately determined after mixing was completed. Simultaneously, the requirements for the pore structure of the test samples and the test process were strictly in accordance with ASTM C457 (ASTM 2016). The low atmospheric pressures were set to 55, 70, 85, and 101 kPa, which are equivalent to the atmospheric conditions of 4,800, 3,000, 1,400, and 0 m above sea level, respectively.

Table 1. Mixture proportions of concrete

Materials	Specific gravities (g/cm^3)	Volumes (L/m^3)
Cement	3.14	134
Sand	2.68	292
Limestone gravel	2.66	406
Water	1	164

Table 2. Admixture contents in different mixture proportions

No.	Water reducer (% by weight of cement)	AEA (% by weight of cement)	Viscosifier (% by weight of cement)	Retarder (% by weight of cement)
Rf1	0.7	—	—	—
Rf2	0.85	—	—	—
Rf3	1	—	—	—
RHP4	1	0.015	—	—
RHP5	1	0.025	—	—
RHP6	1	0.035	—	—
SDS4	1	0.015	—	—
SDS5	1	0.025	—	—
SDS6	1	0.035	—	—
WG7	1	—	0.01	—
WG8	1	—	0.02	—
WG9	1	—	0.03	—
SG10	1	—	—	0.05
SG11	1	—	—	0.1

Fresh Concrete Properties

The properties of fresh concrete were measured via slump, slump flow, air content and V-funnel time in accordance with ASTM C143-15a (ASTM 2015), ASTM C1611-M18 (ASTM 2018), ASTM C138-17a (ASTM 2017), and a reference (Olafusi et al. 2015).

Concrete Pore Structure Tests

The concrete samples were cast in molds that measured 100 × 100 × 100 mm. The samples were demolded approximately 24 h after casting and then cured in a standard curing room at a temperature of 20°C and a humidity of at least 95%. After 28 days of curing, the air-void system parameters were tested in accordance with ASTM C457M-16 (ASTM 2016). Three specimens were tested for each batch.

Pumping Resistance Tests

A pumping resistance tester from the Research Institute of Highway Ministry of Transport of China and Zoomlion Joint Development was used to simulate pumping implementation and to test the pumping resistance of concrete at constant and variable speeds (Ke et al. 2019). A simulation was conducted with reference to the Japan Society of Civil Engineer (JSCE) F509 specification (JSCE 2010) for the deformation evaluation of fresh concrete with a push rate of 12.5 mm/s and an elevation angle of 20° (Fig. 3).

The equipment consists of four parts: a hydraulic unit, an oil cylinder, a cone pipe, and a platform. The piston diameter of the copper cylinder is 155 mm, and its piston length is 1,000 mm. The cylinder has a smooth internal surface, a piston O-ring, and inner

(a)

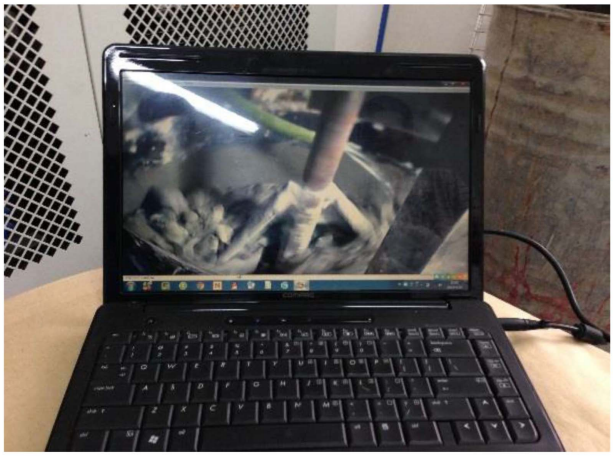

(b)

Fig. 2. Low-atmospheric-pressure test chamber and control device: (a) environmental chamber; and (b) computer control terminal.

surface sealing. The taper pipe, which can be removed from the cylinder, is 500 mm long and has an inner diameter of 100–155 mm. The flange thickness of the copper tube is 10 mm, and the thickness of the copper pipe is 3 mm. The platform, oil cylinder, and taper pipe are connected. The cone is filled with concrete when the pump is operating. The pipe shaft and horizontal directions can be set. Two parameters are obtained by the pumping resistance test: push distance and average push resistance. The range of push distance is 0–1,000 mm. When the final push distance is less than 1,000 mm, pump blockage has occurred. The average push resistance range is 0–2 MPa; the smaller the value is, the smaller the pumping resistance. When the pump is blocked, the average pushing resistance will quickly reach 2 MPa (JSCE F509).

Results and Discussion

Effect of Low Atmospheric Pressure on Concrete Air Entraining

To study the influence of atmospheric pressure value (APV) on the air-entraining performance of concrete, the air content, bubble stability, and pore structure of two different AEAs were compared at varying atmospheric pressures but a fixed mix proportion.

Influence of Atmospheric Pressure on the Air Content of Fresh Concrete

As shown in Fig. 4, the air-entraining capacity of an AEA is weakened to different degrees compared with that at normal pressure (101 kPa) with a decrease in atmospheric pressure, and the final air content of concrete is reduced by not less than 45%. The larger the amount of AEA, the higher the initial air content is, and the greater the air content of concrete decreases with atmospheric pressure. The air content of concrete can decrease by up to 75% of the initial value at normal atmospheric pressure. The air-entraining performance of RHP is slightly better than that of SDS. However, the final air content of concrete is less than 3% in a low-pressure environment.

Influence of Atmospheric Pressure on the Air Content Loss of Fresh Concrete

As shown in Fig. 5, the time-dependent air content of two types of air-entrained concrete in two atmospheric pressure environments (101 and 70 kPa) was compared. The air content of concrete with AEA decreased over time under normal and low pressures. Air content loss is greater at low pressure. However, the RHP air-entrained concrete generally has less time-dependent air content loss, better bubble stability, less than 10% air content loss at normal pressure at 1.5 h, and greater than 3% air content at low pressure at 1.5 h. By contrast, the SDS air-entrained concrete is not only low in initial air content at low pressure, but it also has an air content of only 2.4% at 1.5 h, which does not meet specification requirements.

Influence of Atmospheric Pressure on the Pore Structure of Hardened Concrete

The pore structure of concrete was determined at atmospheric pressures of 101 and 70 kPa using the straight-line method. According to ASTM C457-16, the Standard Test Method for Microscopic Determination of Parameters of the Air-Void System in Hardened Concrete, the air-void parameters in hardened concrete were measured. The formulas for calculating the bubble parameters in hardened concrete are

$$a = A/N \tag{1}$$

where a = average bubble area, μm^2; A = total bubble area; and N = bubble quantity

$$A_s = 100na\,(\%) \tag{2}$$

where A_s = air content; and n = bubble quantity per unit area

$$L = \frac{P}{aA_s}\left(\frac{P}{A_s} < 4.33\right) \tag{3}$$

$$L = 3\left[1.4\left(\frac{P}{A_s} + 1\right)^{1/3} - 1\right]\left(\frac{P}{A_s} > 4.33\right) \tag{4}$$

where L = bubble space coefficient; and P = paste content (%).

The air content, bubble spacing factor, and average pore diameter were obtained as provided in Table 3. The results indicate that the number of bubbles after concrete hardening at low pressure is evidently lower than that at normal pressure with the same amount of AEA. Moreover, the air content of hardened concrete is also significantly lower at low pressure than at normal pressure, which is consistent with the test results of the air content of fresh concrete at different pressures. An insufficient number of bubbles evidently increases the bubble spacing coefficient.

(a)

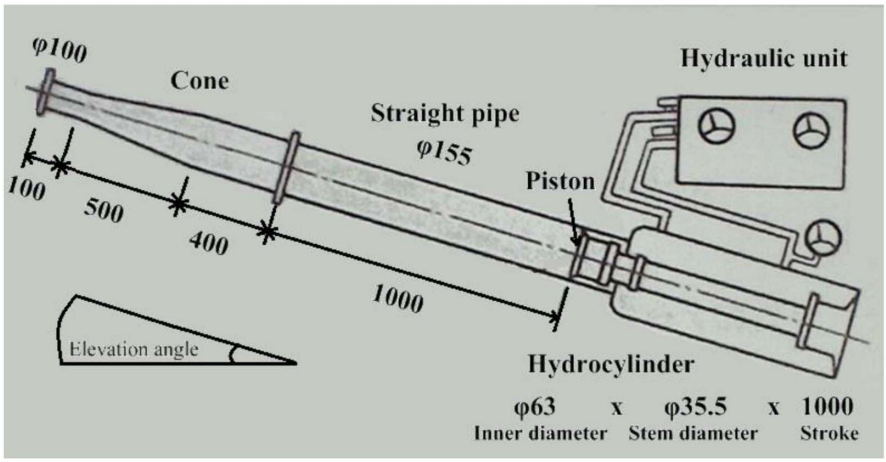

(b)

Fig. 3. Pump resistance tester, operating table, and display screen: (a) pump resistance tester; and (b) schematic diagram of pump resistance tester.

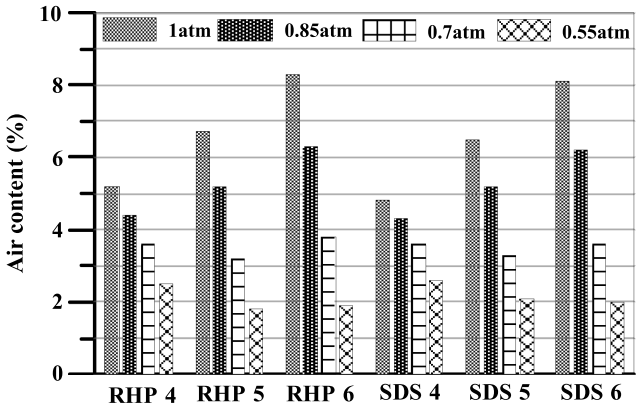

Fig. 4. Air content at different pressures.

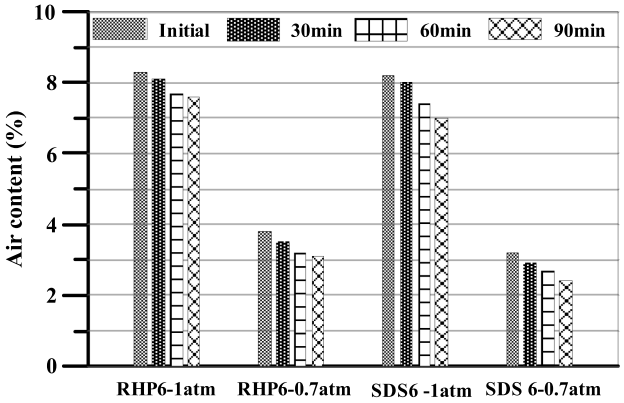

Fig. 5. Changes in air content at different pressures.

Simulated Pumping of Mixed Concrete under Different Atmospheric Pressures

Although the increase in the air content of concrete will reduce the compressive strength to some extent, the pumpability of fresh concrete and the frost resistance of hardened concrete can be improved. The air content of concrete is considerably reduced at low air pressure, which may cause the pumping performance of concrete to deteriorate.

The pumping of concrete requires better workability due to a pipeline flow process under the action of a piston. However, given

Table 3. Concrete pore structure mixed under different atmospheric pressures

AEA	APV (kPa)	Air content (%)	Spacing factor (μm)	Specific area (mm^{-1})	Average diameter (μm)	Number of voids (N)
RHP4	101	5.20	198	25.65	156	715
	70	3.50	327	20.31	197	306
SDS4	101	4.80	173	29.63	135	874
	70	3.60	348	19.61	204	301

Table 4. Workability and pumping resistance of concrete mixed at normal pressure

Item	Rf1	Rf2	Rf3	RHP4	RHP5	RHP6	WG7	WG8	WG9	SG10	SG11
Slump (mm)	150	185	200	230	180	140	190	180	150	210	215
Slump flow (mm)	190	270	300	445	275	235	230	200	180	445	410
V-funnel time (s)	100	25	20	25	50	80	35	37	40	40	45
Average resistance (MPa)	1.436	1.158	0.957	0.573	0.497	0.738	0.632	0.657	0.723	0.643	0.668

that a concrete production plant requires a certain transportation time to reach the construction site, the concrete mixture may lose slump while in transit when a traffic jam occurs or when the destination is far away (Ding et al. 2001). Consequently, fluidity will drop and pumping will be impossible. At present, additives used in pumping concrete available on the market mostly consist of components such as water-reducing agents, AEAs, retarders, and viscosities (Vosahlik et al. 2018). To determine the pumpability of concrete at low atmospheric pressure, the relationships among the concrete slump, slump flow, air content, V-funnel time, and average pumping pressure are compared at 1 and 0.55 atm (1 atm = 101,325 Pa). The composition of each pumping agent changes. The mixture proportions are provided in Tables 1 and 2, and the relevant results are presented in Table 4 and Figs. 6–9.

Simulated Pumping Test at Normal Pressure

Table 4 indicates that with the same type of admixture, concrete V-funnel tests exhibit considerable correlation with slump and slump flow, concrete with a large slump, a large slump flow, and a short V-funnel time. This result may be attributed to the slump, slump flow, and V-funnel time, demonstrating the macroscopic performance of concrete under its own weight, such as the yield stress value and the segregation resistance (Olafusi et al. 2015) of the concrete. From Rf1 to RHP4, RHP5, and RHP6, the slump and slump flow of concrete initially increase significantly and then decrease slightly as the amount of AEA increases from zero. Meanwhile, from Rf1 to RHP4, RHP5, and RHP6, the V-funnel time of concrete initially decreases significantly and then increases slightly. The simulated pumping average resistance of concrete also exhibits a similar trend(i.e., initially decreasing and then increasing). However, both values are considerably smaller than those of concrete without AEA. Therefore, a conclusion can be drawn that the use of AEA is an effective method for reducing pumping resistance. However, if the air content of concrete is too high, then the average pumping resistance increases. The reason for this finding may be related to the plastic viscosity of concrete. A certain amount of air-inducing bubbles will reduce the plastic viscosity of concrete; however, an optimal value exists. If the air content is too large, then the plastic viscosity will increase (Ren et al. 2015).

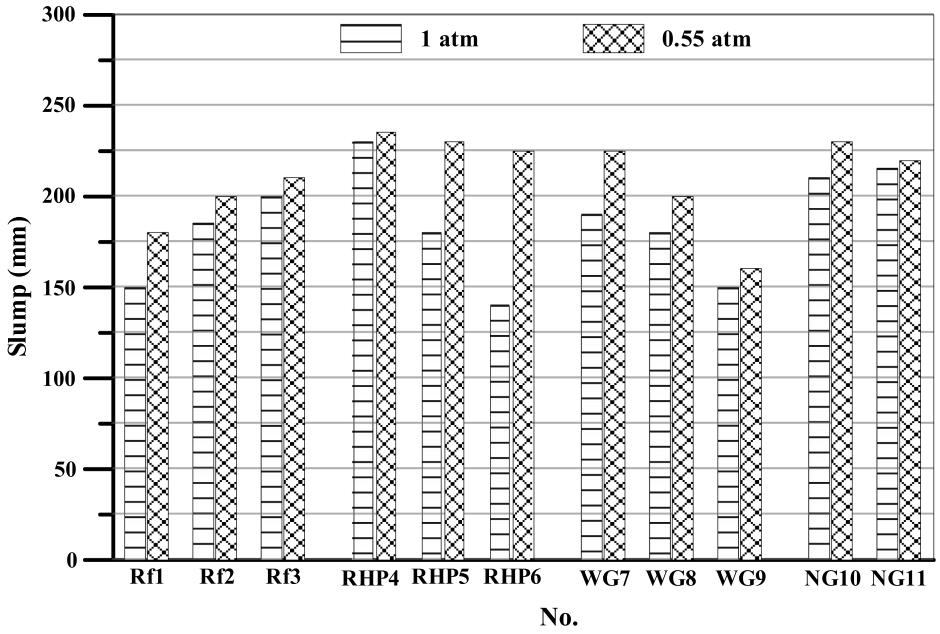

Fig. 6. Slump at different pressures.

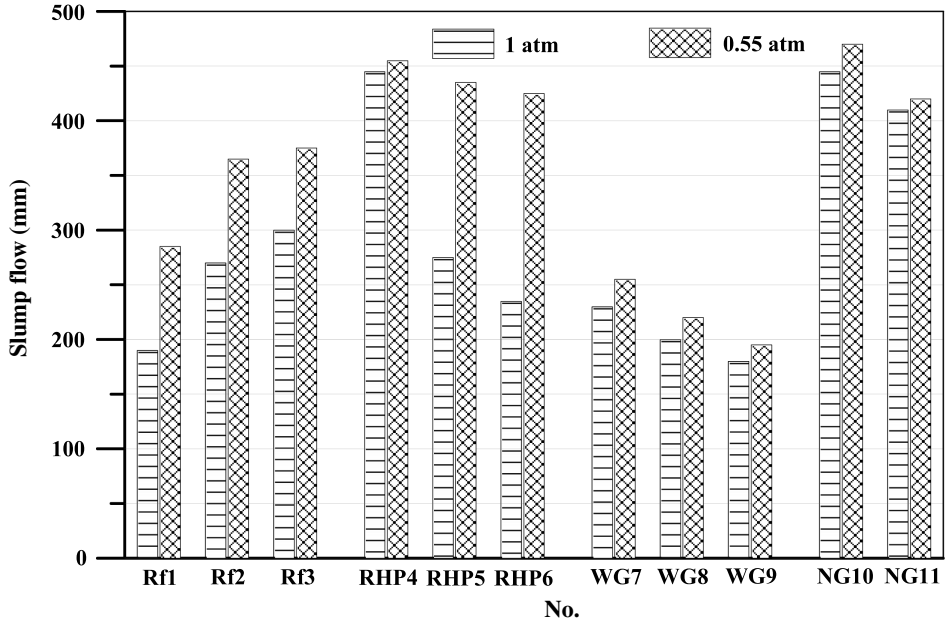

Fig. 7. Slump flow at different pressures.

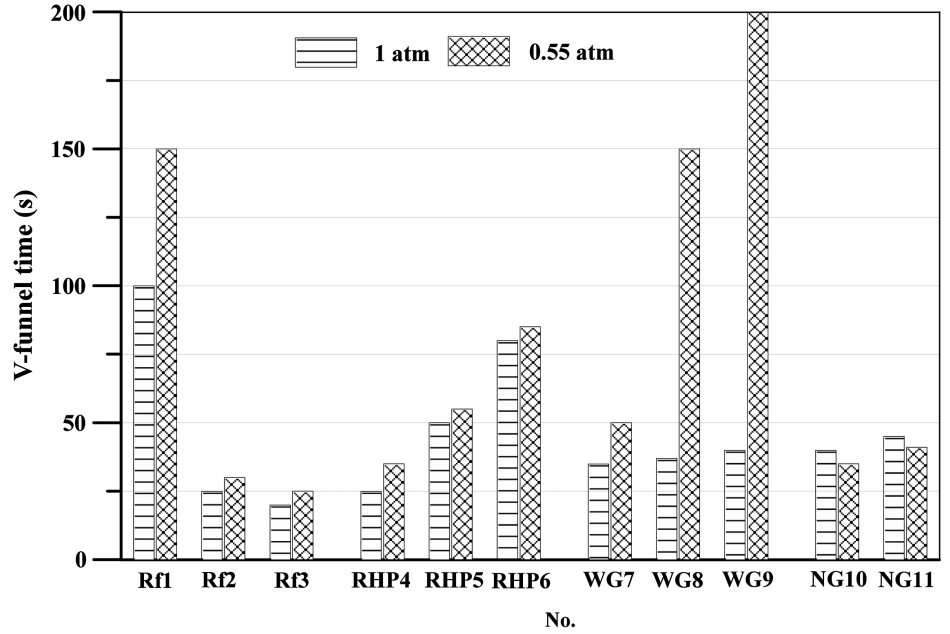

Fig. 8. V-funnel time at different pressures.

In the 11 sets of simulated pumping tests listed in Table 4, the average pumping pressure of RHP5 is the smallest, whereas that of Rf1 is the largest. With an increase in the amount of water-reducing agent, the Rf series concrete exhibits improved fluidity, slump, slump flow, and V-funnel time and reduced pumping resistance. The WG series exerts a considerable influence on the air content of concrete, and the pumping resistance is significantly reduced. However, the average pumping resistance of WG7 is not the smallest. The SG series exhibits a relatively remarkable improvement in fluidity, while the average pumping resistance drops significantly.

Certain limitations exist when judging the pumpability of concrete via slump, slump flow, and V-funnel time. For concrete with a large slump and a short V-funnel time, the pumping resistance is not necessarily small. The use of air-entraining bubbles is a more effective means of reducing pumping resistance. The final average pumping pressure of concrete is the result of a comprehensive reflection of each indicator.

Simulated Pumping Test at Low Pressure

Figs. 6 and 7 and Table 4 show that the slump and slump flow of concrete increase under low-pressure conditions compared with those under normal pressure conditions. However, the effects of different admixture components vary.

Under normal pressure conditions, the slump of concrete increases from 150 to 200 mm with an increase in water-reducing

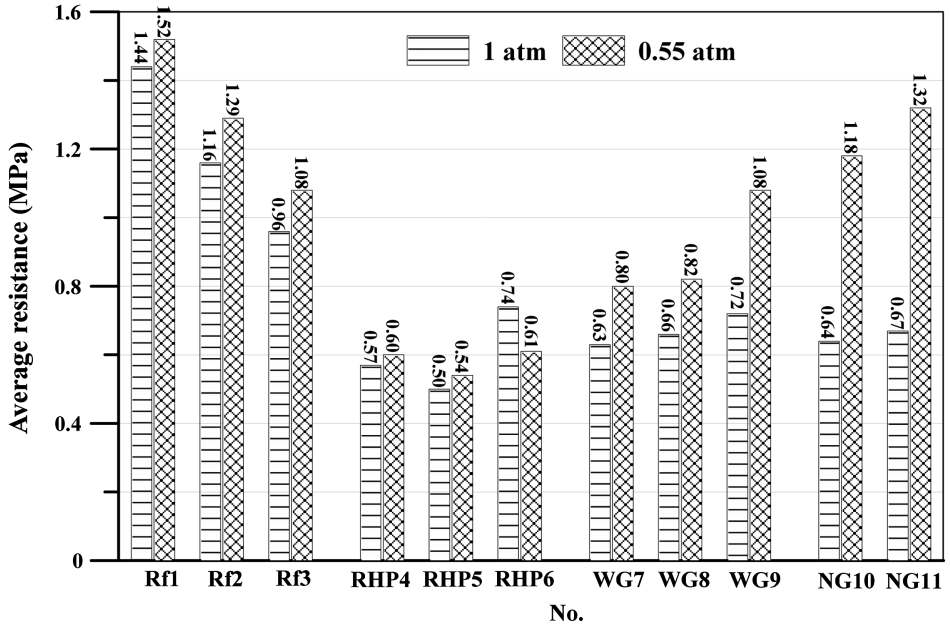

Fig. 9. Pumping resistance at different pressures.

agent dosage, and slump flow increases from 190 to 300 mm. Under low-pressure conditions, the slump of concrete increases from 180 to 210 mm with an increase in the water-reducing agent dosage, and the slump flow increases from 285 to 375 mm.

Under normal pressure conditions, the slump and slump flow of concrete decreased considerably with an increase in AEA amount. This finding may be attributed to air entraining increasing the yield stress value of concrete (Ke et al. 2015). Air content will directly affect concrete workability (i.e., slump and slump flow). Since air content varies with air pressure, it is expected that slump/slump flow values would change accordingly. Under low-pressure conditions, the higher the content of AEA, the greater the increase in slump and slump flow of concrete. This finding may be attributed to the significant decrease in the air-entraining capacity of AEA under low-pressure conditions. The lower the air-entraining effect is, the smaller the air content, the smaller the yield stress, and the greater the slump and slump flow.

As shown in Fig. 8, the water-reducing agent is increased to a certain extent, and the V-funnel time of concrete is rapidly reduced. The relationship between the WG amount and V-funnel time is insensitive under normal pressure conditions. The V-funnel time of concrete with a water-reducing agent, AEA, and WG will increase under low-pressure conditions. Among them, the V-funnel time of concrete with WG will increase significantly, whereas that of concrete with SG will be appropriately reduced.

A comparison of pumping resistance at normal pressure and low pressure is shown in Fig. 9. The atmospheric pressure is reduced from 1 atm to 0.55 atm, the average pumping resistance of concrete is increased to a certain extent, and pumpability deteriorates. The increase range varies under the action of different admixtures. Concrete with a water-reducing agent exhibits an increase in pumping resistance value of 5.9%–12.4% at low pressure. Concrete with AEA presents the least increase in pumping resistance at low pressure (i.e., less than 10%). The increase in pumping resistance of concrete with WG is between 26.4% and 49.3% at low pressure. The increase in pumping resistance of concrete with SG at low pressure is the highest (i.e., over 80%). The use of WG and SG under low-pressure conditions increases the difficulty of concrete pumping.

Mechanism Analysis

The air content of air-entrained concrete declines sharply with a decrease in atmospheric pressure, and the maximum reduction exceeds 75% of the initial air content. The air content loss of air-entrained concrete is intensified at low pressure, and the prepared concrete is unlikely to meet the air content antifreezing requirement. The air content of hardened air-entrained concrete is reduced in a low-pressure environment, the bubble spacing factor is increased, and the bubble structure deteriorates. This result may be attributed to the mass of bubbles per unit volume in concrete being considerably reduced in a low-pressure environment. Moreover, the density of the concrete, except for the bubbles, does not differ from that at normal pressure and the buoyancy of bubbles inside the concrete is high. Consequently, the stability of the bubbles deteriorates during the dynamic balance process and the bubbles easily agglomerate and collapse, which eventually leads to low air content in concrete, numerous large pores, and pore structure deterioration.

Specifically, this can be calculated by the formulas in Eqs. (5)–(12) and described by Fig. 10.

For ideal gas, there are formulas in Eqs. (5)–(8)

$$PV = nRT \tag{5}$$

$$m = nM \tag{6}$$

$$m = V\rho \tag{7}$$

$$\rho = PM/RT \tag{8}$$

In concrete, the acceleration of bubbles, $m_{\text{bubble}}\alpha$, can be calculated by Eq. (9)

$$m_{\text{bubble}}\alpha = \rho_{\text{concrete}}V_{\text{bubble}}g - m_{\text{bubble}}g - V_{\text{bubble}}\beta \tag{9}$$

Using Eqs. (7)–(9), α can be calculated by Eq. (10)

$$\alpha = (\rho_{\text{concrete}}/\rho_{\text{bubble}} - 1)g - \beta/\rho_{\text{bubble}} \tag{10}$$

where ρ_{concrete} = density of concrete from which bubbles are removed; m_{bubble} = mass of the bubbles; V_{bubble} = volume of the

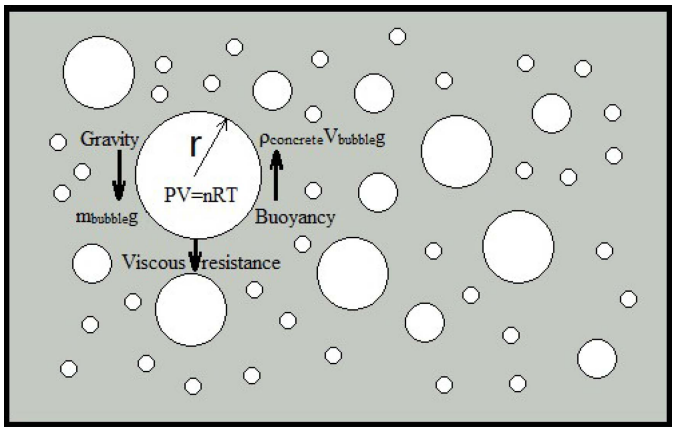

Fig. 10. Schematic diagram of the acceleration calculation for bubbles in concrete.

bubbles; ρ_{bubble} = density of the bubbles; g = gravity acceleration; β = drag coefficient; and β multiplied by V_{bubble} = viscous resistance of bubbles in concrete. The $\rho_{concrete}$ of ordinary concrete is generally greater than 2,400 kg/m^3, and the ρ_{bubble} of bubbles at 1 atm is 1.29 kg/m^3, so $\rho_{concrete}/\rho_{bubble} \gg 1$, and α can be calculated by Eq. (11)

$$\alpha \approx (\rho_{concrete} g - \beta)/\rho_{bubble} \tag{11}$$

When $\rho_{concrete} g \leq \beta$ and $\alpha \leq 0$, the bubbles are in a stable state; when $\rho_{concrete} g > \beta$ and $\alpha > 0$, the bubbles are in an accelerated state of floating. Gravity acceleration decreases by 0.03% for every 1,000 m increase in altitude (Bray et al. 1995), so when the atmospheric pressure is lowered from P_0 to P_1, $g_1/g_0 \approx 1$. Generally, both $\rho_{concrete}$ and β are parameters that are independent of atmospheric pressure. Using Eqs. (8) and (11), α_1 can be calculated by Eq. (12)

$$\alpha_1 = (P_0/P_1)[(\rho_{concrete} g_1 - \beta)/(\rho_{concrete} g_0 - \beta)]\alpha_0 \approx (P_0/P_1)\alpha_0 \tag{12}$$

where α_0 = bubble acceleration when the altitude is 0 m; atmospheric pressure is P_0; and α_1 = bubble acceleration when the atmospheric pressure is P_1 at high altitude. When the atmospheric pressure is lowered, the acceleration of the bubbles floating in the concrete is greatly increased, and the stability drastically deteriorates.

The slump and slump flow of concrete increased to a certain extent with a decrease in APV. The V-funnel time was prolonged, the average pumping resistance increased, and the influence of different components varied. Concrete with AEA exhibits the largest change in slump and slump flow under low pressure [from Figs. 11(a and b)]. Concrete with WG has a prolonged V-funnel time at low pressure, and the pumping degradation of concrete with SG is the most severe, probably because low pressure changes the air content and bubble structure of the concrete. Consequently, the air-entraining bubbles of the system will affect the rheology of the concrete, which in turn affects the slump, slump flow, V-funnel time, and average pumping resistance.

Conclusions

In this study, the air-entraining and pumping characteristics of high-altitude concrete were tested by simulating low atmospheric pressure and pumping resistance methodologies. Combined with the ideal gas state equation, the air-entraining mechanism of high-altitude concrete was explained. The following conclusions can be drawn.

1. At a constant AEA dosage, the air content of air-entrained concrete declines sharply at low atmospheric pressure, and the maximum reduction exceeds 75% of the initial air content. The air content loss of air-entrained concrete increases with a decrease in atmospheric pressure. The air content of hardened air-entrained concrete decreases with low atmospheric pressure and the pore spacing coefficient increases.
2. There are some limitations in judging the pumpability of concrete by slump, slump flow, and V-funnel time. For concrete with a large slump and slump flow but a short V-funnel time, the average pumping resistance may be large. With an increase in AEA amount, the slump and slump flow of concrete initially increases and then decreases, the V-funnel time initially decreases and then increases, and the average pump pressure of concrete initially decreases and then increases. All the average pump pressures of concrete with AEA are smaller than those of concrete without AEA, and air-entraining bubbles are an effective method for reducing the pumping resistance of concrete.
3. In most cases, the effect of AEA decreases in high-altitude areas, the air content of concrete is significantly reduced, and pumpability deteriorates. An appropriate air-entraining bubble

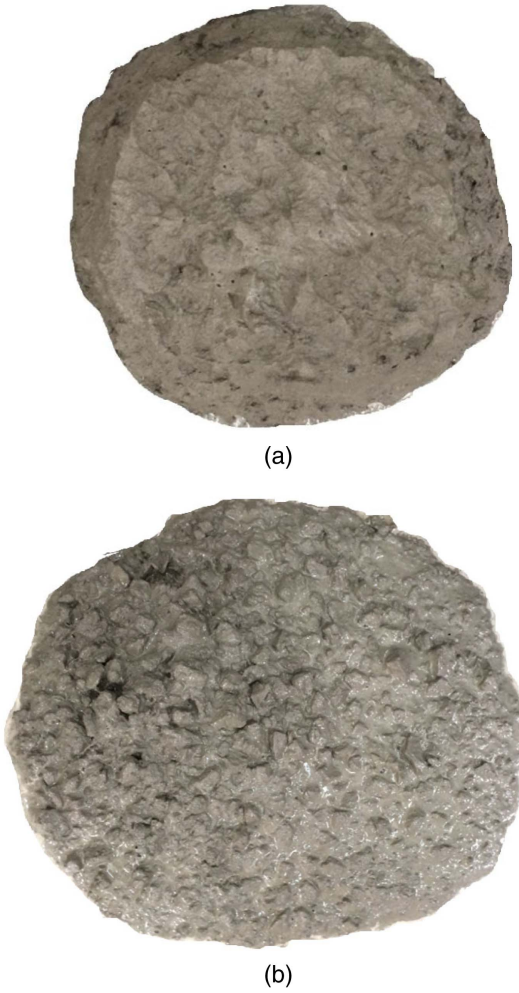

Fig. 11. Morphology of fresh concrete under different pressures: (a) normal pressure; and (b) low pressure.

content is necessary to improve the pumpability of air-entrained concrete. In the process of blending other admixture components, the characteristics of low-pressure concrete should be considered and the strategy used should be changed to avoid the occurrence of pump blockage.

Data Availability Statement

Some or all data, models, or code generated or used during the study are available from the corresponding author by request.

Acknowledgments

The authors gratefully acknowledge the financial support received from the National Natural Science Foundation of China (Grant No. 51308264).

References

ASTM. 2015. *Standard test method for slump of hydraulic cement concrete*. ASTM C143M-15a. West Conshohocken, PA: ASTM.

ASTM. 2016. *Standard test method for microscopical determination of parameters of the air-void system in hardened concrete*. ASTM C457M-16. West Conshohocken, PA: ASTM.

ASTM. 2017. *Standard test method for density (unit weight), yield, and air content (gravimetric) of concrete*. ASTM C138M-17a. West Conshohocken, PA: ASTM.

ASTM. 2018. *Standard test method for slump flow of self-consolidating concrete*. ASTM C1611M-18. West Conshohocken, PA: ASTM.

Bray, A., G. Barbato, and F. Franceschini. 1995. "The effect of gravity acceleration on non-automatic weighing systems." *Measurement* 15 (4): 261–272. https://doi.org/10.1016/0263-2241(95)00011-9.

Dhanapal, S. V., and P. Nanthagopalan. 2020. "Investigations on the influence of binders toward rheological behavior of cementitious pastes." *J. Mater. Civ. Eng.* 32 (3): 04019374. https://doi.org/10.1061/(ASCE)MT.1943-5533.0003038.

Ding, Q. J., S. G. Hu, and B. J. Guan. 2001. "Application of large-diameter and long-span micro-expansive pumping concrete filled steel tube arch bridge." *J. Wuhan Univ. Technol. Mater. Sci.* 16 (4): 73–76.

Feys, D., K. H. Khayat, A. Perez-Schell, and R. Khatib. 2015. "Prediction of pumping pressure by means of new tribometer for highly-workable concrete." *Cem. Concr. Compos.* 57 (Mar): 102–115. https://doi.org/10.1016/j.cemconcomp.2014.12.007.

Georgiadis, A. S., K. K. Sideris, and N. S. Anagnostopoulos. 2010. "Properties of SCC produced with limestone filler or viscosity modifying admixture." *J. Mater. Civ. Eng.* 2 (4): 352–360. https://doi.org/10.1061/(ASCE)MT.1943-5533.0000030.

Hazaree, C. V., and V. Mahadevan. 2016. "Single-stage pumping of concrete up to 2.432 km (1.51 miles): Admixture, mixture, and full-scale trials." *J. Mater. Civ. Eng.* 28 (11): 05016002. https://doi.org/10.1061/(ASCE)MT.1943-5533.0001446.

He, T. S., and Y. Y. Hu. 2006. "Effect of sodium gluconate in pumping agent on concrete performance." [In Chinese.] *Concrete* 198 (4): 32–33.

Jacobsen, S., L. Haugan, T. A. Hammer, and E. Kalogiannidis. 2009. "Flow conditions of fresh mortar and concrete in different pipes." *Cem. Concr. Res.* 39 (11): 997–1006. https://doi.org/10.1016/j.cemconres.2009.07.005.

JSCE (Japan Society of Civil Engineers). 2010. *Test method for deformability of fresh concrete using a pumping tester*. JSCE F509. Tokyo: JSCE.

Ke, G., J. Wang, and B. Tian. 2019. "Simulation analysis of pumping and its variability for manufactured sand concrete." *ACI Mater. J.* 116 (3): 35–42. https://doi.org/10.14359/51714504.

Ke, G., and J. Zhang. 2020. "Effects of retarding admixture, superplasticizer and supplementary cementitious material on the rheology and mechanical properties of high strength calcium sulfoaluminate cement paste." *J. Adv. Concr. Technol.* 18 (1): 17–26. https://doi.org/10.3151/jact.18.17.

Ke, G., J. Zhang, S. Xie, and T. Pei. 2020. "Rheological behavior of calcium sulfoaluminate cement paste with supplementary cementitious materials." *Constr. Build. Mater.* 243 (May): 118234. https://doi.org/10.1016/j.conbuildmat.2020.118234.

Ke, G. J., B. Tian, and J. L. Wang. 2015. "Effects of air-entraining agents and welan gum on rheological properties of fresh cement mortar." In *Proc., 14th Int. Congress on the Chemistry of Cement*. Beijing: Chinese Ceramic Society.

Kim, J. H., S. H. Kwon, S. Kawashima, and H. J. Yim. 2017. "Rheology of cement paste under high pressure." *Cem. Concr. Compos.* 77 (Mar): 60–67. https://doi.org/10.1016/j.cemconcomp.2016.11.007.

Li, X., Z. Fu, and Z. Luo. 2015. "Effect of atmospheric pressure on air content and air void parameters of concrete." *Mag. Concr. Res.* 67 (8): 391–400. https://doi.org/10.1680/macr.15.00057.

Liu, J., K. Wang, Q. Zhang, G. R. Lomboy, L. Zhang, and J. Liu. 2020. "Effects of ultrafine powders on the properties of the lubrication layer and highly flowable concrete." *J. Mater. Civ. Eng.* 32 (5): 04020099. https://doi.org/10.1061/(ASCE)MT.1943-5533.0003193.

Olafusi, O. S., A. P. Adewuyi, A. I. Otunla, and A. O. Babalola. 2015. "Evaluation of Fresh and Hardened Properties of Self-Compacting Concrete." *Open J. Civ. Eng.* 5 (1): 1–7. https://doi.org/10.4236/ojce.2015.51001.

Ren, W.-Y., B. Tian, G.-J. Ke, and X.-Y. He. 2015. "Experimental study on rheological property of air-entrained cement mortar." [In Chinese.] *J. Highway Transp. Res. Dev.* 32 (8): 29–33. https://doi.org/10.3969/j.issn.1002-0268.2015.08.006.

Vosahlik, J., K. A. Riding, D. Feys, W. Lindquist, L. Keller, S. Van Zetten, and B. Schulz. 2018. "Concrete pumping and its effect on the air void system." *Mater. Struct.* 51 (4): 1–15. https://doi.org/10.1617/s11527-018-1204-1.

Wu, B. X., B. G. Chen, J. H. Xu, and M. Z. Kang. 2011. "Analysis of pumping pressure loss law of high strength and high-performance concrete." [In Chinese.] *Concrete* 255 (1): 142–144.

Yazdani, N., M. Bergin, and G. Majtaba. 2000. "Effect of pumping on properties of bridge concrete." *J. Mater. Civ. Eng.* 12 (3): 212–219. https://doi.org/10.1061/(ASCE)0899-1561(2000)12:3(212).